IMAGE REPRESENTATION IN ITERATIVE IMAGE RECONSTRUCTION BASED ON HIGH ORDER EVEN POLYNOMIAL WINDOWS

Marek Jaskuła and Wojciech Chlewicki*

* Szczecin University of Technology

Marek.Jaskula@ps.pl

Abstract: Image representation plays a significant role in image reconstruction from projections using iterative methods. In this work two iterative image reconstruction methods, in which the solution was represented using a linear combination of polynomial windows, were evaluated. The methods were algebraic reconstruction technique (ART) and row-action maximum likelihood algorithm (RAMLA). Novel basis functions were compared to recently used blobs introduced by Lewitt. The evaluation based on simulated data showed that polynomial windows and Lewitt's blobs achieved comparable results. This happened for both ART and RAMLA.

Introduction

Iterative image reconstruction has been shown to be preferable approach in many cases such as computed tomography, nuclear medicine, microscopy and nondestructive evaluation over analytical approach. Despite being computationally demanding as compared to analytical methods iterative algorithms offer several advantages and can be applied even in complex image reconstruction tasks including volumetric imaging [1]. Crucial facet of iterative reconstruction methods determining their performance is possibly accurate forward/backward projection operator. This strictly depends on the way the discrete image is represented in the computer.

Intuitive approach of representing such images by a finite number of parameters is through dividing the image into pixels. Pixel has a unit value inside a small square and has zero value outside. This simple representation, however, due to its inherent lack of smoothness leads to inaccurate calculation of projections of the represented image and is not satisfactory for image reconstruction from projections.

Alternatives to pixels for image representation in iterative reconstruction algorithms have been proposed [2], [3], [4], [5]. Instead image is represented using basis functions which decay to zero within increasing distance. In this case the images are constructed as the sum of scaled and shifted copies of an image element which overlap. Thus the image value is well defined for every point in the image despite the fact that it is represented only by a finite set of numbers.

Several kernels have been proposed in the literature as basis functions. Andersen and Kak suggested bilinear elements [6] whereas Hanson and Wecksung [3] presented study using B-splines. The Gaussian function has been also considered in iterative image reconstruction by the latter authors [3] as well as by Snyder et al [7] and Schweiger and Arridge [5].

Presently, the most common basis functions utilized in iterative reconstruction methods are based on the generalized Bessel-Kaiser window used in signal processing. This family of image elements, called blobs, have been introduced into the field of image reconstruction by Lewitt [8], [9]. Their main advantage is that they are band-limited with a possibility of easy tuning and that there is a convenient formula for computing the projection of those basis functions.

As an option a family of polynomial windows was evaluated in this work. The initial results of utilizing polynomial windows as basis functions for iterative image reconstruction were presented in [10]. The coefficient values of polynomial windows were optimized in such a way as to follow the requirements suggested for blobs. Those are accuracy of the reconstruction and ability to form an accurate approximation to a constant-valued function of the spatial variables.

Materials and methods

The image representation $\hat{f}(x,y)$ utilized here is constructed as the superposition of scaled and shifted copies of the basis function Φ

$$\hat{f}(x,y) = \sum_{j=1}^{J} c_j \Phi(x - x_j, y - y_j) \tag{1}$$

where $\{(c_j)\}_{j=1}^{J}$ is a set of coefficients of the image representation and $\{(x_j, y_j)\}_{j=1}^{J}$ is a set of J points in 2D space that are the nodes of a uniform grid over a region of the space.

The blob formula proposed by Lewitt has the following form [9]

$$bl_{m,T,\alpha}(r) = \frac{1}{I_m(\alpha)} (\sqrt{1-(r/T)^2})^m I_m(\alpha \sqrt{1-(r/T)^2}) \tag{2}$$

for $0 \leq r \leq T$ and value zero for $r > T$, where r is the radial distance from the blob center. I_m denotes the modified Bessel function of order m, T is the radius of the blob and α is a parameter controlling the blob shape.

 ISSN: 1727-1983

A general formula for computing the polynomial counterpart of that basis function can be defined as follows

$$bp_{T,D}(r) = 1 + \sum_{k=1}^{D} a_{2k} \left(\frac{r}{T}\right)^{2k} \quad (3)$$

where T is the extent of the basis function and D is a half of the polynomial extension degree.

From the equation (1) the line integral $\hat{p}_i$ of $\hat{f}$ along the line integral i has the form

$$\hat{p}_i = \sum_{j=1}^{J} a_{ij} c_j \quad (4)$$

where a_{ij} is the line integral, along the line i, of the shifted basis function with the center in (x_j, y_j). Since the considered basis functions are spherically symmetric a_{ij} is independent on the angular orientation of the line of integration and depends only on the distance r of the line from the center of the basis function.

Projection of the Lewitt kernel (Abel transform) is proportional to $b_{m+1/2,T,\alpha}(r)$ and can be analytically computed in a convenient way [8]

$$pl_{m,T,\alpha}(r) = \quad (5)$$

$$= \frac{a}{I_m(\alpha)} \sqrt{\frac{2\pi}{\alpha}} \left(\sqrt{1-\left(\frac{r}{T}\right)^2}\right)^{m+1/2} \cdot I_{m+1/2}\left(\alpha\sqrt{1-\left(\frac{r}{T}\right)^2}\right)$$

A general formula for the Abel transform of the polynomial window is presently being introduced by Jaskuła [11]

$$pp_{T,D}(r) = \quad (6)$$

$$= \sqrt{T^2-r^2} \sum_{j=0}^{D} r^{2j} \sum_{k=j}^{D} 2\, \frac{a_{2k}\left(-T^2+r^2\right)^{k-j} k!\, (-1)^{k+j}}{T^{2k}(2k-2j+1)\,(k-j)!\, j!}$$

As observed by Matej and Lewitt [12] basis functions can accurately represent the constant function when the Fourier transform of the basis function is zero at all multiples of the "sampling" frequency of the image-space grid. For $\alpha = 10.8$ the Lewitt kernel have the first zero crossing of the kernel spectrum at the sampling frequency. Optimized coefficients of the polynomial window which follow the same properties as the blobs were found and are presented in table 1. Spatial and frequency characteristics of the windows described above are shown in figure 1. In figure 2 the projections of those windows are plotted.

The forward/backward projections were implemented in the form of a footprint based ray driven splatting [13]. The footprint table [3],[12] had dimension 200 for the basis function radius 2.0 relative to the grid increment. The iterative image reconstruction algorithms used in this study were algebraic reconstruction technique (ART) [14] and row-action maximum likelihood algorithm (RAMLA) [15]. The number of iterations was set 5 for both methods. The relaxation coefficient for ART was experimentally chosen 0.07 whereas the values of the coefficient for RAMLA was subsequently 0.71, 0.31, 0.14, 0.09 and 0.06 in each iteration.

Table 1: Optimised coefficients of the polynomial window which follow the properties of the blobs with presented α.

Coeff.	$\alpha = 10.8$
a_0	1.0000
a_2	-6.3710
a_4	18.4145
a_6	-32.1102
a_8	37.7124
a_{10}	-31.0969
a_{12}	17.7065
a_{14}	-6.3124
a_{16}	1.0571

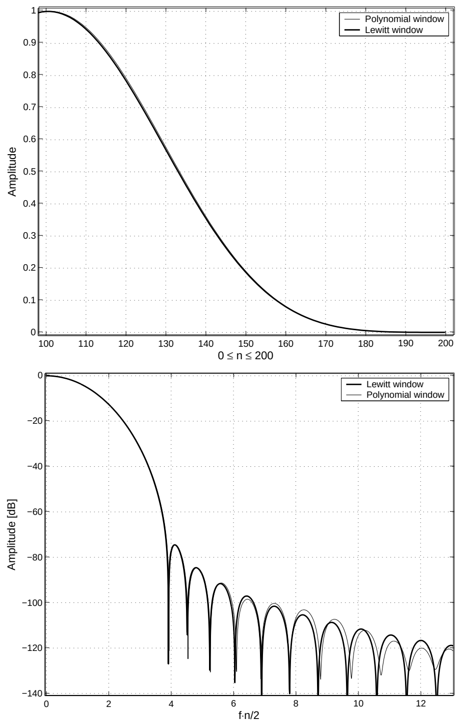

Figure 1: Radial profile (up) and frequency characteristics (down) of the Lewitt kernel ($\alpha = 10.8$, radius equal to 2) and its polynomial counterpart.

For the purpose of evaluation projections of the Shepp-Logan head phantom [16] and the custom phantom with high contrast spots of a different shape and radius were generated using software simulator [17]. For the first phantom he simulated data consisted of projections taken at 90 equally spaced angles within 180 degrees arc. For the second phantom the number of angular orientations was 45. In the first case the projection size was equal to 129 whereas in the second case the size was 65. In both cases the image size was equal the projection size.

Results

The reconstructed images of the phantoms using RAMLA with polynomial window are depicted in Figure 2. The rest of images represent the difference between the reconstruction and the original phantom. So that, the distribution of the errors within each image can be visible more clearly.

In Figure 3 difference images are shown between the original phantom and its reconstruction using ART. Left images present utilization of Lewitt window whereas right images show employing the polynomial window.

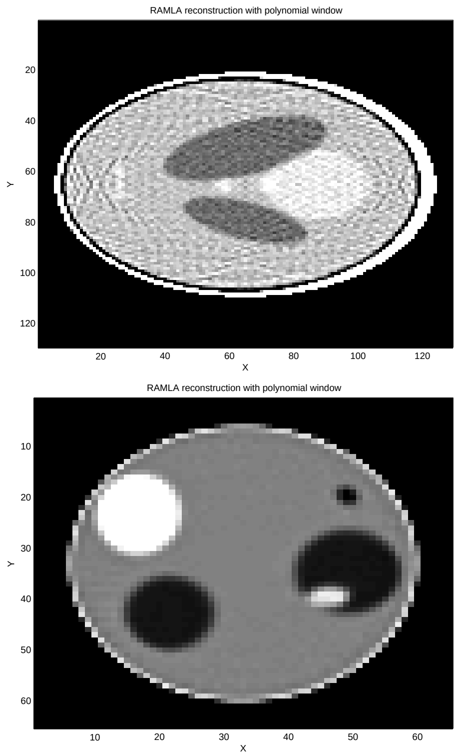

Figure 2: Reconstructions of two phantoms using RAMLA with the polynomial basis function.

In figure 4 the difference images are presented. The upper image visualize the spatial distribution of the error between the digitized phantom and the reconstruction. Observing the difference image between the reconstruction utilizing the Lewitt kernel and that with the polynomial window (figure 4 down) it can be concluded that the methods produce ripples of different nature (due to diverse in shape shape and frequency characteristics of each blob - figure 1) and there is a difference in a way they handle streaking artifacts. More thorough study is needed considering that matter which will be performed in the future.

Conclusions

The effect of different basis expansions of the reconstructed images for two iterative image reconstruction

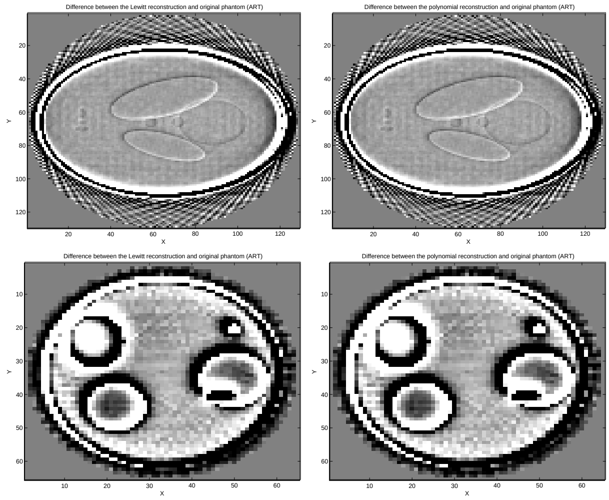

Figure 3: Difference images between the original phantom and its reconstruction using ART. Left images present utilization of Lewitt window whereas right images show employing the polynomial window.

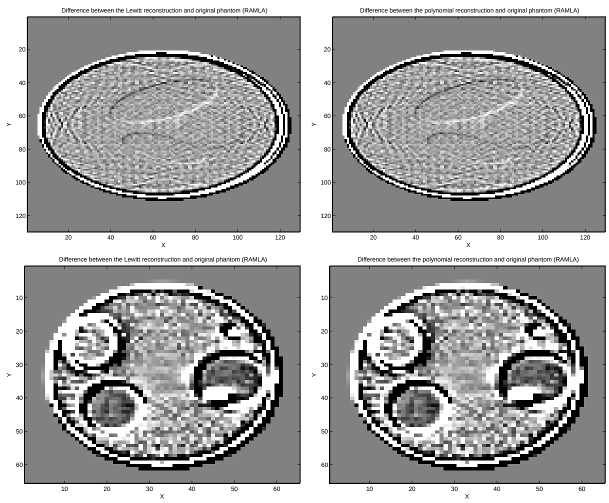

Figure 4: Difference images between the original phantom and its reconstruction using RAMLA. Left images present utilization of Lewitt window whereas right images show employing the polynomial window.

methods was investigated. The evaluation based on simulated data showed that polynomial windows and Lewitt's blobs achieved comparable results. This happened for both ART and RAMLA.

Regarding future investigations it seems that iterative image reconstruction methods with the basis functions based on the polynomial window could be investigated using methodology presented by Donaire and Garcia [18].

Further on, there is a need for investigation of the appropriate image reconstruction quality criteria. Some of the possibly useful measures where describe in [19]. It has to be investigated to which degree optimization of the basis functions has positive impact of the image quality. This will justify choosing more sophisticated basis function instead of pixels.

References

[1] CHLEWICKI, W. BADEA, C., AND PALLIKARAKIS, N. (2001): 'Cone based 3D reconstruction: A FDK-SART comparison for limited number of projections', In *MEDICON 2001*, Pula, Croatia

[2] CENSOR, Y. (1983): 'Finite series-expansion reconstruction methods', *Proceedings of the IEEE*, **71**,pp. 409–419

[3] HANSON, K. M. AND WECKSUNG, G. W. (1985): 'Local basis-function approach to computed tomography', *Applied Optics*, **24**,pp. 4028–4039

[4] HERMAN, G.T. AND LENT, A. (1976): 'Iterative reconstruction algorithms', *Comput. Biol. Med.*, **6**,pp. 273–294

[5] SCHWEIGER, M. AND ARRIDGE, S.R. (2003): 'Image reconstruction in optical tomography using local basis functions', *Jour. of Electronic Imag.*, **12**,pp. 583–593

[6] ANDERSEN, A.H. AND KAK, A.C. (1984): 'Simultaneous Algebraic Reconstruction Technique(SART): a superior implementation of the ART algorithm', *Ultrason. Img.*, **6**, pp. 81–94

[7] SNYDER, D.L., MILLER, M.I., THOMAS, L.J., AND POLITTE, D.G. (1987): 'Noise and edge artifacts in maximum-likelihood reconstruction for emission tomography', *IEEE Trans. Med. Imag*, **3**,pp.228–237

[8] LEWITT, R. M. (1990): 'Multidimensional digital image representation using generalized Kaiser-Bessel window functions', *J. Opt. Soc. Am. A*, **7**, pp. 1834–1846

[9] LEWITT, R. M. (1992): 'Alternatives to voxels for image representation in iterative reconstruction algorithms', *Phys. Med. Biol.*, **37**, pp. 705–716

[10] CHLEWICKI, W. AND JASKUŁA, M. (2004): 'Image representation in iterative image reconstruction based on polynomial windows', In *Int. Conf. on Signals and Electronics systems*, Poznan, Poland, pp. 297–300

[11] JASKUŁA, M. (2004): 'The polynomial window and its Abel transform', In *Int. Conf. on Signals and Electronics systems*, Poznan, Poland, pp. 301–304

[12] MATEJ, S. AND LEWITT, R. M. (1996): 'Practical considerations for 3-D image reconstruction using spherically symmetric volume elements', *IEEE Trans. Med. Imag.*, **15**,pp. 68–78

[13] MUELLER, K., YAGEL, R., AND WHELLER, J.J. (1999): 'Fast implementations of algebraic methods for the 3D reconstruction from cone-beam data', *IEEE Trans. Med. Imag.*, **18**,pp. 538–547.

[14] GORDON, R., BENDER, R., AND HERMAN, G.T. (1970): 'Algebraic Reconstruction Techniques (ART) for three-dimensional electron microscopy and x-ray photography', *J. Thoery Bio.*, **29**,pp. 471–481

[15] BROWNE, J. AND DE PIERRO, A.R. (1996): 'A row-action alternative to the EM algorithm for maximizing likelihoods in emission tomography', *IEEE Trans. Med. Imaging*, **15**, pp. 687–699

[16] KAK, A. C. AND SLANEY, M. (1988): *'Principles of Computerized Tomographic Imaging'*, IEEE Press.

[17] TOFT, P. (1996): *'The Radon transform - theory and implementation'*, PhD thesis, Technical University of Denmark, Lyngby, Denmark

[18] DONAIRE, J.G. AND GARCIA, I. (2002): 'On using global optimization to obtain better performance of a MART algorithm in 3D X-ray tomography', *Jour. of Imag. Sci. Technol.*, **46**, pp. 247–256.

[19] HERMAN, G.T. AND YEUNG, K.T.D. (1989): 'Evaluators of image reconstruction algorithms'. *International J. Imaging Systems Technol.*, **1**, pp. 187–195